Published in final edited form as:
J Neuroimmunol. 2014 September 15; 274(0): 86–95. doi:10.1016/j.jneuroim.2014.06.016.

Selective expression of Narp in primary nociceptive neurons: role in microglia/macrophage activation following nerve injury

M Miskimon[1], **S Han**[2], **JJ Lee**[2], **M Ringkamp**[3], **MA Wilson**[1], **RS Petralia**[4], **X Dong**[1], **PF Worley**[1], **JM Baraban**[1,2], and **IM Reti**[1,2,5]

[1]Department of Neuroscience, Johns Hopkins University

[2]Department of Psychiatry, Johns Hopkins University

[3]Department of Neurosurgery, Johns Hopkins University

[4]NIDCD, NIH

[5]laboratory of origin

Abstract

Neuronal activity regulated pentraxin (Narp) is a secreted protein implicated in regulating synaptic plasticity via its association with the extracellular surface of AMPA receptors. We found robust Narp immunostaining in dorsal root ganglia (DRG) that is largely restricted to small diameter neurons, and in the superficial layers of the dorsal horn of the spinal cord. In double staining studies of DRG, we found that Narp is expressed in both IB4- and CGRP-positive neurons, markers of distinct populations of nociceptive neurons. Although a panel of standard pain behavioral assays were unaffected by Narp deletion, we found that Narp knockout mice displayed an exaggerated microglia/macrophage response in the dorsal horn of the spinal cord to sciatic nerve transection 3 days after surgery compared with wild type mice. As other members of the pentraxin family have been implicated in regulating innate immunity, these findings suggest that Narp, and perhaps other neuronal pentraxins, also regulate inflammation in the nervous system.

Keywords

pain; AMPA; dorsal root ganglion; CGRP; pentraxin; inflammation

INTRODUCTION

Members of the pentraxin family of proteins are expressed in a variety of tissues and mediate innate immunity and inflammation (Garlanda et al, 2005; Bottazzi et al, 2006). All

Correspondence should be addressed to: Irving Reti, MBBS, Associate Professor, Psychiatry and Neuroscience, Johns Hopkins University, 600 N. Wolfe St., Meyer 3-181, Baltimore, MD 21205, Phone: 410-955-1484, Fax: 410-955-0152, imreti@jhmi.edu.

members of this family share a conserved pentraxin domain but can be divided into two subgroups called “short” and “long” pentraxins, with the latter containing N-terminal extensions prior to the pentraxin domain located in their C-terminal portion. The prototypic “short” pentraxin, C-reactive protein (CRP) is an acute phase reactant which precipitates from human serum upon addition of the C-polysaccharide of pneumococcus (Tillet et al 1930, Marnell et al, 2005). PTX3, a “long” pentraxin, was originally identified as a novel protein induced by tumor necrosis factor in human fibroblasts and later found to be regulated by inflammatory cytokines in a number of cell types, including macrophages and dendritic cells (Lee et al, 1990; Lee et al 1993). Three “long” pentraxins, Narp, NP1 and NPR, are highly enriched in the nervous system, where they are selectively expressed in neurons, and are therefore referred to as neuronal pentraxins. The neuronal pentraxins are secreted at synapses, cluster AMPA receptors by binding to their extracellular surface and have been implicated in synaptic plasticity and synaptogenesis (O’Brien et al., 1999; Xu et al., 2003; Cho et al., 2008). However, it is unclear if neuronal pentraxins also play a role in regulating immune function or if the function of this branch of the pentraxin family is restricted to regulating AMPA receptor trafficking.

Although AMPA receptors are expressed ubiquitously throughout the nervous system, individual neuronal pentraxins display highly heterogeneous patterns of expression. For example, Narp is localized selectively to dentate granule cells in the hippocampus (Reti et al., 2002b), to the anterdorsal nucleus in the thalamus (Reti et al., 2002a), and to a small subset of neurons in the hypothalamus, including orexin and vasopressin neurons (Reti et al., 2002c; Reti et al., 2008a). As part of a survey of Narp expression in the nervous system, we identified Narp expression in dorsal root ganglia (DRG), where it appeared to be expressed predominantly in small diameter neurons, characteristic of primary nociceptive neurons. These neurons send axons to the dorsal horn of the spinal cord where they transmit nociceptive signals by release of glutamate which acts on AMPA and other glutamate receptor subtypes (Nagy et al, 2004). Enhanced AMPA receptor signaling in the spinal cord has been implicated in pain sensitization (hyperalgesia) and allodynia in which benign stimuli become painful (Tao, 2010). Accordingly, we evaluated the effect of deleting Narp on acute and chronic models of mechanical, thermal, and inflammatory pain. Then, we performed sciatic nerve transection, an injury known to induce robust glial activation in the spinal cord, to assess differences in inflammatory response between Narp knockout (KO) and control mice.

MATERIALS AND METHODS

Animals

Generation of Narp KO mice has been described elsewhere (Johnson et al., 2007; Reti et al., 2008b). All control and KO mice used in these studies were generated by heterozygote breeding pairs that had been backcrossed to C57BL/6 for five generations. Both male and female mice were used between 9–14 weeks of age. Mice were used for all experiments except the rhizotomy study which was conducted with Sprague–Dawley rats obtained from Charles River (Wilmington, MA, USA). Rodents were maintained on a 12-h light/dark cycle and were given access to food and water *ad libitum*. Experiments complied with the NIH

guidelines for animal care and were approved by the Johns Hopkins University Institutional Animal Care and Use Committee. Every effort was made to minimize the number of animals used and their suffering.

Antibodies

The following primary antibodies were used: rabbit anti-Narp antibody (O'Brien et al., 1999), guinea pig anti-CGRP (Peninsula Laboratories, San Carlos, CA), rabbit anti-Iba1 (Wako Chemicals USA Inc, Richmond, VA), rabbit anti-NF200 (Chemicon, Billeria, MA), mouse anti-peripherin (Chemicon), and mouse anti-BrdU (Sigma-Aldrich, St. Louis, MO). In addition, we used a fluorochrome-conjugated isolectin B4 lectin (IB4; Molecular Probes, Carlsbad, CA) which binds non-peptidergic DRG neurons.

Immunoblot analysis

DRG were solubilized by sonication for 10s in a solution of 0.1% Triton X-100 with protease inhibitors (aprotinin and leupeptin, each at 1 μg/mL, and 1 mM phenylmethylsulphonyl fluoride) in PBS (pH - 7.4). Following sonication, samples were spun down at 14,000x*g* in a microcentrifuge for 5 minutes at 4°C to remove insoluble material. Protein concentrations were determined using amido black colorimetric protein assay.

Solubilized DRG lysates were mixed with an equal volume of Laemmli Sample Buffer (Bio-Rad; Hercules, CA). Equal concentrations of protein were separated by SDS-PAGE (10% acrylamide) at 130V for 60 minutes. Proteins were electrophoretically transferred to nitrocellulose paper. Blots were blocked with 3% nonfat milk in TBS and Tween-20 (TBS-T; 20 mM Tris (pH -7.7), 137mM NaCl and 0.05% Tween-20) overnight at 4°C. Narp antibody was diluted in blocking buffer (1:5000) and blots were incubated overnight at 4°C. Blots were washed repeatedly (6 times) in TBS-T for 5 minutes. HRP-conjugated anti-rabbit secondary antibody was diluted in blocking buffer and blots were incubated overnight at 4°C. Blots were washed in TBS-T for 5 minutes, 3 times, and then in TBS for 5 minutes, 3 times. Immunoblots were processed for protein visualization using enhanced chemiluminescence (Amersham Pharmacia Biotech Inc; Piscataway, NJ) and exposed to Biomax-MR film (Kodak; Rochester, NY).

Tissue section staining

Mice were anesthetized with chloral hydrate (400mg/kg, i.p., Sigma Aldrich) and perfused via the left ventricle with 4% paraformaldehyde. The vertebral column containing spinal cord and DRG was carefully dissected from each mouse and incubated overnight at 4°C in 4% paraformaldehyde before being switched to 25% sucrose made in PBS and allowed to incubate for an additional 2 days. Tissue sections (20μm) were cut on a sliding microtome, placed on frosted glass microslides, air dried, and washed in PBS. Sections were incubated in 10mM sodium citrate (pH 8.5) in 80 C water bath for 30 minutes. They were then cooled to room temperature and washed with PBS. Sections were blocked in 3% BSA and 0.3% Triton-X 100 made in PBS for one hour before incubation overnight with primary antibodies at the following dilutions: Narp (1:5000), CGRP (1:500), Iba1 (1:500), peripherin (1:1000), NF200 (1:1000). Fluorochrome-conjugated IB4 lectin was used at 1:500. After washing in

PBS, the sections incubated in primary antibodies were incubated with either a fluorochrome-labeled (cy3; 1:200) or biotinylated secondary antibodies (1:500; Jackson; West Grove, Pa) against the species in which the primary antibodies were generated. Slides processed with antibody complexes containing fluorochrome-labeled secondary antibodies or IB4 lectin were washed in PBS and cover-slipped. Antibody complexes containing biotinylated secondary antibodies were further processed with avidin-linked biotinylated peroxidase and exposed to tyramide for fluorescent visualization. For quantification of double-labeling with Narp and either CGRP, IB4, peripherin or NF200, we used 3–6 mice for each marker and ascertained the mean percentage of Narp–positive cells that stain for the other marker based on 4 representative DRG sections from each mouse.

Electron microscopy

Immunogold studies of Narp localization were performed as described previously (Reti et al., 2008a). Briefly, mice were perfused with 4% paraformaldehyde with 0.5% glutaraldehyde and sections of tissue were frozen in liquid propane in a Leica CPC cryopreparation chamber and then freeze-substituted into Lowicryl HM-20 in a Leica AFS. Ultrathin sections on grids were incubated in 0.1% sodium borohydride plus 50 mM glycine in Tris-buffered saline plus 0.1% Triton X-100 (TBST), followed by 10% normal goat serum (NGS) in TBST. Both sides of the sections were then incubated with rabbit anti-Narp (1/50–1/67) and guinea pig anti-CGRP (1/100) antibodies mixed together in 1% NGS/TBST overnight at 4°C. After several washing and blocking steps, the secondary immunogold antibodies (goat F(ab)2 anti-rabbit IgG:5 nm gold and goat anti-guinea pig IgG:15 nm gold; BB International Gold, distributed by Ted Pella, Redding, CA, USA) in 1% NGS/TBST plus 0.5% PEG (20,000 MW) were applied to both sides of the sections for 1 hr at room temperature. Finally, sections were stained with uranyl acetate and lead citrate. Figures were processed in Adobe Photoshop with minimal use of levels; brightness and contrast were employed uniformly over the images. Omission of primary antibodies yielded negligible staining.

Hot-water tail immersion test

Noxious thermal stimulation was produced by immersing the tip of the mouse tail into a hot-water bath. The hot-water bath was adjusted to maintain a temperature of 50.0°C ± 0.2. After allowing acclimation in a clean cage identical to the home cage for a period of 30 minutes, the posterior one-third of the tail of each animal was immersed in the water bath until rapid removal of the tail was observed, signifying a pain response. The cut-off time was 15 seconds to avoid tissue damage.

Hargreaves model of thermal hyperalgesia

Thermal hyperalgesia was measured in a manner similar to that described by Hargreaves et al. (1988). After allowing acclimation atop a glass surface underneath 5 cm x 15 cm plexiglass containers, the plantar surface of the hind paw of each mouse was exposed to a high-intensity projector light source before and after injection of 3μl, 6μl, and 12 μl of 1:1 solution of Complete Freund’s Adjuvant (CFA) and normal saline. The light source was directed onto the plantar surface of the hindpaw until withdrawal was observed, signifying a

pain response. Cutoff time was 20 seconds to avoid tissue damage. Measurements were performed 24 hours before, and 1, 24, 48, 72 and 96 hours after injection of CFA.

Hotplate Test

Hotplate testing was performed in a manner similar to that described by Woolfe and MacDonald (1944). The plate was adjusted to maintain a temperature of 54.0°C ± 0.2. After allowing acclimation outside the home cage for 30 minutes, each animal was placed individually onto the surface of the hotplate until the animal licked its paw, noticeably flinched its paw or jumped, signifying a pain response. Cut-off time was 30 seconds to avoid tissue damage.

Spared Nerve Injury

Under ketamine-xylazine anesthesia, the skin on the lateral surface of the thigh was shaved. After a small incision was made in the skin, blunt dissection of the biceps femoris muscle was used to expose the sciatic nerve and its three terminal branches: the sural, common peroneal and tibial nerves. The spared nerve injury consisted of severing the common peroneal and tibial nerves while leaving the sural nerve intact, taking care not to damage or stretch the sural nerve. Muscle was closed with 5.0 silk and the skin was closed with a single staple.

Mechanical allodynia

Mechanical allodynia was assessed in a manner described by Descosterd and Woolf (2000). After placing mice on an elevated wire grid and allowing acclimation for 30 minutes, the medial and lateral plantar surfaces of the hind paw were stimulated with a series of von Frey monofilaments with ascending force beginning at 0.002 g. The paw withdrawal threshold was the lowest force that elicited a paw withdrawal to one of five applications of the von Frey filaments.

Sciatic nerve transection

Under ketamine-xylazine anesthesia the skin on the lateral surface of the thigh was shaved and incised. Blunt dissection was performed through the biceps femoris muscle to expose the common sciatic nerve. The sciatic nerve was severed and a 0.5 mm segment was removed to prevent the two nerve ends growing together. Muscle was closed with 5.0 silk and the skin was closed with a single staple. Control mice were shaved and an incision was made over the thigh. However, the sciatic nerve was not exposed and the wound was closed with a single staple. Mice were sacrificed either approximately 48 or 72 hours after surgery.

Quantification of microglia/macrophage activation

For quantifying microglia/macrophage activation, we used the proportional area method (Donnelly et al., 2009; Fatemi et al., 2011) to determine the proportion of the ventral or dorsal horn that was Iba1-positive. In addition, we also monitored Iba1-positive cell counts in these regions. Firstly, the L4 -5 spinal cord segment from littermate pairs was identified by following root filaments of the L4 through L6 dorsal root ganglia. Spinal cord sections from each littermate pair were placed on either end of a single slide and processed for Iba1

immunohistochemistry. A representative section was chosen from each animal and microglia/macrophage quantification was performed blind to genotype. Whole spinal cord sections were visualized through a 5x objective and digitally captured by a Zeiss microscope fitted with a Retiga 2000R camera (QImaging Surrey, BC Canada) for quantification by the Iba1-positive proportional area method. To quantify cell numbers, we used a 20x objective to visualize cells in the dorsal and ventral horns. Images were captured using IPLab (Scanalytics Inc., Rockville, MD) and quantified using MCID Core (Interfocus Imaging Ltd, Linton, Cambridge, England). To quantify using both the Iba1-positive proportional area method and cell counts, we used an identical sized rectangle just large enough to encompass the dorsal or ventral horns. Each image from the littermate pair was subjected to identical contrast adjustment so that cells were clearly visible in both sections.

To apply the proportional area method to quantify Iba1 staining, we first determined the threshold level of intensity below which is considered background and above which is categorized as Iba1-positive staining. Threshold was determined using images of the contralateral ventral horn, the area which had the lowest Iba1 staining making it easier to distinguish between background and Iba1-positive pixels. To determine the threshold for Iba1-postive staining, all the pixels above a given intensity value were highlighted. This intensity value was adjusted to find the highest value at which all the pixels that were clearly part of microglia/macrophage profiles were included. In this way, threshold values were determined for the sections from each littermate pair. The average threshold value obtained for each littermate pair using the contralateral ventral horn was then applied to images from the other three areas (ipsilateral dorsal and ventral horns, contralateral dorsal horn) analyzed in sections from that littermate pair. The staining intensity in the sections from naive mice was separately quantified in the same manner, using the ventral horn as reference for the threshold.

To threshold the images used to quantify cell counts, we used the ipsilateral dorsal horn which had the highest intensity staining, so that we could easily distinguish cells in these images. As above, threshold was set as the highest intensity value such that all Iba1-positive cell bodies were included. Once threshold values for each of the two sections from each littermate pair were obtained, the average threshold value was applied to both images. Dots consisting of fewer than forty pixels were excluded to help distinguish individual cells. Images of the ipsilateral ventral horn, contralateral dorsal horn, and ventral horn were processed in the same manner using thresholding established for the ipsilateral dorsal horn. The cell counts in the sections from naive mice were separately quantified in the same manner, using the dorsal horn as reference for the threshold.

Analysis of microglia/macrophage proliferation

To label proliferating microglia/macrophages in the spinal cord after sciatic nerve transection, we used the thymidine analogue 5-bromo-2’-deoxyuridine (5-BrdU, Sigma-Aldrich). The mice received an intraperitoneal injection of BrdU (100mg/kg, 20mg/ml in 10% DMSO) immediately before sciatic nerve transection. Following surgery, the mice were injected with BrdU daily for three days, including two hours before perfusion. The L4–5 spinal cord sections were made as described above.

For double-label immunohistochemistry, sections were first pre-treated with 50% formamide in 2x standard saline citrate (SSC) in 65 C water bath for 2 hours, followed by 30 minutes in 2N HCl at 37 C and 10 minutes in 0.1M sodium borate buffer. They were blocked in 1% BSA + 0.3% Triton-X 100 + 3% normal donkey serum made in TBS for one hour. Sections were incubated overnight in antibodies against Iba1 (1:500) and BrdU (1:1000). Staining was completed as described above.

The ipsilateral dorsal and ventral horns were visualized through a 10x objective and digitally captured by a Zeiss microscope equipped with AxioCam MRm. As for quantifying microglia/macrophage activation, we used an identical sized rectangle over each section just large enough to encompass the ventral or dorsal horns. One representative section from each animal was selected for quantifying what percent of Iba1-positive cells were also positive for BrdU in the dorsal and ventral horns ipsilateral to the lesion. The contralateral dorsal and ventral horns had negligible numbers of BrdU-positive cells which were not quantified.

Quantification of monocyte chemotactic protein-1 (MCP-1)

Mice were sedated with chloral hydrate (400 mg/kg, i.p., Sigma-Aldrich) and then decapitated with a small animal guillotine. After rapid identification and removal of the L4-L6 spinal cord segment, it was frozen on dry ice, and stored at -80°C. Total RNA from the harvested tissue samples was extracted in an RNase-free environment using Qiagen miRNeasy Mini Kit (Qiagen; Valencia, CA) and was quantified by Nanodrop (Johns Hopkins Deep Sequencing & Microarray Core Facility; Baltimore, MD). Total RNA (100ng) was converted into cDNA with oligo$(dT)_{20}$ primers in 20 μL reactions using the iScript Select cDNA Synthesis Kit (Bio-Rad). Subsequent quantitative real-time polymerase chain reaction (qPCR) was performed with iQ SYBR® Green Supermix (Bio-Rad) on an iQ Multicolor Real-Time PCR Detection System (Bio-Rad). To normalize samples, we monitored levels of the housekeeping gene, glyceraldehyde-3-phosphate dehydrogenase (GAPDH). The primer sequences were MCP-1 forward (gtccctgtcatgcttctggg), MCP-1 reverse (tgaggtggttgtggaaaaggtag), GAPDH forward (tgtgtccgtcgtggatctga) and GAPDH reverse (cctgcttcaccaccttcttga). For each animal, the cDNA from a single reverse transcription reaction was used for both MCP-1 and GAPDH quantification. All samples were run in triplicate and the average threshold cycle (C) for GAPDH was subtracted from that for MCP-1 in each animal.

RESULTS

Expression of Narp in dorsal root ganglia and spinal cord dorsal horn

We observed robust Narp staining in a subpopulation of DRG neurons (figure 1A). Staining was almost completely confined to small and medium sized neurons. Consistent with Narp expression in primary nociceptive neurons in DRG and with previous studies demonstrating that Narp is selectively targeted to axons (Reti et al., 2002b,c), we also found strong Narp staining in laminae I and II of the dorsal horn (figure 1B). In addition, we noted a few, scattered Narp cell bodies in deeper layers of the dorsal horn.

To assess the specificity of this staining pattern, we processed DRG and spinal cord sections from WT and Narp KO mice for immunostaining in parallel. In contrast to the striking heterogeneous pattern of Narp staining observed in DRG and spinal cord sections from WT mice, corresponding sections from Narp KO mice display a low level of diffuse staining, presumably reflecting increased non-specific staining in KO sections (figure 1A' and 1B').

To investigate the specificity of the Narp antibody used for immunostaining studies, we also processed DRG lysates from WT and KO mice (figure 1C). Narp forms high molecular weight (>400 kD), SDS-resistant, complexes which are made up of aggregates of hexameric complexes (O'Brien et al., 1999; Reti and Baraban, 2000). DRG immunoblotting reveals a robust, slowly migrating band that corresponds to high molecular weight Narp aggregates which is completely absent in KO lysates.

Dorsal rhizotomy reduces Narp staining in dorsal horn

To assess whether Narp staining in the dorsal horn reflects expression in terminals of nociceptive afferent neurons, we checked whether rhizotomy would reduce Narp staining in the dorsal horn of rat. Accordingly, we performed rhizotomy at levels L4 to L6 and then processed spinal cord sections for immunostaining 14 days later, to allow for clearance of degenerated terminals. This procedure reduced the level of Narp staining in the dorsal horn at L5 on the side ipsilateral to surgery (figure 1D). As a positive control, we processed sections for CGRP staining, which is also reduced, as expected (figure 1D'). In contrast, the T12 segment of the spinal cord showed comparable Narp (figure 1E) and CGRP (figure 1E') expression on both sides indicating this region is unaffected by rhizotomy at L4 to L6. Of note, the reduction of CGRP terminal staining at L5 appears to be more complete than that of Narp terminals, suggesting that Narp terminals may also arise from other sources aside from DRG. This observation is consistent with previous studies demonstrating that Narp is prominently expressed in orexin neurons (Reti et al., 2002c) which also send projections to the dorsal horn (Date et al., 2000; Guan et al., 2003).

Narp-positive neurons are primarily restricted to small-diameter neurons of the DRG

Small and medium diameter DRG neurons that have unmyelinated or lightly myelinated axons can be identified immunohistochemically by staining for peripherin, a type III intermediate filament, while medium and large diameter DRG neurons that have heavily myelinated axons can be identified by staining for NF200, a heavy-chain neurofilament (Lawson and Waddell, 1991). To help classify Narp-positive neurons, we performed double-label immunohistochemical studies on DRG sections with Narp and either NF200 or peripherin. We found that 91±2.5% of Narp-positive neurons express peripherin while only 8±2.3% of Narp-positive neurons express NF200 (figure 2A,B,E). Conversely, we found that 76 ±3.5% of peripherin-positive neurons express Narp. As Narp is an immediate early gene that can be induced by neuronal activation (Tsui et al., 1996; Reti and Baraban, 2000), we also checked if injections of complete Freund's adjuvant (CFA) or formalin given peripherally might alter Narp levels in the DRG as determined by immunoblotting. However, we did not find that to be the case in samples harvested up to 3 days after CFA or formalin injection (data not shown). Spinal nerve transection was not associated with elevated DRG Narp levels either (data not shown)

Cellular distribution of Narp-positive neurons in mouse DRG

Small-diameter nociceptive neurons of the DRG can be further subdivided into nerve growth factor (NGF)-sensitive and glial cell line-derived neurotrophic factor (GDNF)-sensitive subtypes, which can be distinguished immunohistochemically by expression of calcitonin gene-related peptide (CGRP), a marker of peptidergic neurons, and by isolectin B4 (IB4) binding, a marker of non-peptidergic neurons (Molliver et al, 1997). To assess whether Narp is expressed in either of these subpopulations, we performed double-labeling studies on DRG sections with Narp antibody and either CGRP antibody or IB4 lectin binding. We found that Narp is expressed in both types of nociceptive neurons as 29±3.2% of Narp-positive neurons also stain for CGRP, and 39±7% of Narp-positive neurons bind IB4 lectin (figure 2C,D,E). Examination of DRG sections double-stained for CGRP and Narp revealed that the degree of double-labeling varied markedly with the size of the CGRP neurons. Large CGRP neurons were infrequently Narp-positive, whilst approximately one-third of small and medium sized CGRP neurons expressed Narp (data not shown).

Narp-positive terminals in the dorsal horn

In the dorsal horn, terminals of peptidergic nociceptive neurons are restricted to lamina I and the outer layer of lamina II (IIo) while those of the non-peptidergic neurons are confined to the central layer of lamina II (IIc). Double-label immunohistochemical studies of mouse spinal cord sections demonstrate that Narp immunoreactive terminals also extend to the level of IB4-binding lamina IIc (figure 3A,B). Narp terminals (figure 3C) and puncta (figure 3C') also overlap with CGRP (figure 3D,D'), indicating expression of Narp in layers lamina I and lamina IIo. To obtain direct evidence that Narp is expressed in terminals of nociceptive afferent neurons that terminate in the dorsal horn, we conducted double labeling studies for Narp and CGRP on sections processed for electron microscopy. As expected, we found examples of Narp and CGRP labeling in the same nerve terminal (figure 3E).

Pain assessment in Narp KO mice

As Narp is predominantly expressed in small DRG neurons responsible for nociceptive signal transduction, we checked whether Narp contributes to this response by assessing pain-related behavior in Narp KO mice. We performed three established assays for assessing acute thermal nociception: the hotplate test, Hargreaves test and the hot water tail-immersion test (Allen and Yaksh, 2004a,b). We did not find differences in baseline pain behavior with the 54°C hotplate test, the Hargreaves test or the 50°C hot-water tail immersion test (figure 4).

Inflammatory pain and neuropathic pain responses in Narp KO mice

We also checked whether Narp deletion alters recovery from inflammatory or neuropathic pain. CFA injection into the paw is an established model for generating chronic inflammatory pain. We injected three different volumes of reagent (1:1 CFA:normal saline) and assayed the induction and recovery of inflammatory pain using the Hargreaves test. Both WT and Narp KO mice exhibited similar induction and recovery profiles (figure 5A).

We used the spared nerve injury (SNI) model to induce neuropathic pain behavior in mice and screened for development of a hyperalgesic pain response using von Frey filaments.

Following SNI, the intact sural nerve exhibits increased sensitivity, which can be assessed with mechanical stimulation (von Frey filaments) of the non-injured skin territory (Decosterd and Woolf, 2000). We found no significant differences in the baseline responses or the induction of hyperalgesia between WT and Narp KO mice up to 96 hours after SNI surgery (figure 5B).

Microglia/macrophage response following sciatic nerve transection

In addition to surveying pain behavior, as described above, we also evaluated inflammatory response following sciatic nerve transection (SNT). SNT induces a robust microglia/macrophage response beginning as early as 1 day after the procedure, with maximal activation occurring 2 to 4 days after surgery in rats and 3 to 5 days after surgery in mice (He et al, 1997; Liu et al, 2000). We chose to compare microglia/macrophage activation between WT and Narp KO mice 3 days after performing SNT, using Iba1 staining to monitor microglia/macrophage activation. In both WT and Narp KO mice, we observed enhanced Iba1 staining in the dorsal horn on the side ipsilateral to the lesion (figure 6A and B). However, Iba1 staining intensity and the complexity of process ramification in the dorsal horn of Narp KO mice appeared greater than in the same region of WT mice. Accordingly, we quantified Iba1 staining intensity in the ipsi- and contralateral dorsal and ventral horns and found it to be 66% higher in the ipsilateral dorsal horn of Narp KO mice compared with the same region of WT controls ($p<0.01$, paired Student's t-test; figure 6C). There is also a trend towards greater Iba1 staining intensity in the ventral horn of Narp KO compared with WT mice. In addition, we checked Iba1-positive cell counts in the same regions and found that Narp KO mice have 52% more microglia/macrophages in the dorsal horn ipsilateral to the lesion than WT mice ($p<0.05$, by paired Student's t-test; figure 6D). Narp deletion did not affect Iba1 staining intensity or cell count on the side contralateral to the lesion. Nor did Narp deletion affect baseline Iba1 levels. Iba1 staining in naive WT (figure 6E) and Narp KO (figure 6F) mice is comparable and appears similar to levels in the contralateral dorsal and ventral horns of the mice that underwent SNT, although a direct comparison was not possible as the sections were processed at different times. However quantification of Iba1 staining intensity and cell counts in naive Narp KO (n=4) and WT (n=4) mice revealed no significant differences (data not shown).

Next, we performed double-label immunostaining for BrdU and Iba1 to assess whether the increase in microglia/macrophages is due to increased proliferation of these cells. In both WT and Narp KO mice, approximately two thirds of all Iba1-positive cells in the dorsal horn ipsilateral to the lesion were also positive for BrdU. There was no significant difference in the percentage of BrdU-positive microglia/macrophages between the Narp KO (n=4) and the WT control (n=4) mice (data not shown).

As MCP1 contributes to microglial activation after peripheral nerve injury (Zhang et al., 2007), we checked whether Narp deletion alters its expression after SNT (figure 7). Spinal cord samples were harvested from the same levels of the spinal cord that display Iba1 induction immunohistochemically. As we had performed Iba1 staining studies 3 days following SNT, we monitored MCP1 mRNA levels by qPCR in samples harvested from naïve mice and in those harvested on either the second or third days after SNT. Two-way

ANOVA revealed a main effect of surgery ($F(2,30)=53.503$, $p<0.0001$), however there was no effect of genotype ($F(1,30)=0.832$, $p=0.369$) nor an interaction effect ($F(2,30)=0.884$, $p=0.424$). Post-hoc analyses did not detect significant differences in MCP1 level by genotype in either naïve mice or at the day 2 or day 3 time points ($ps>0.62$).

DISCUSSION

In this study we report constitutive Narp expression in a subset of primary nociceptive neurons. This restricted pattern of Narp expression in a subpopulation of DRG neurons fits with its heterogeneous expression pattern previously observed in other brain regions. For example, in the hippocampus, Narp is selectively expressed in dentate granule cells (Reti et al., 2002b). In the hypothalamus, Narp is only expressed in a small population of neurons, including orexin and vasopressin neurons (Reti et al., 2002c and 2008a). We also observed Narp terminal staining in the dorsal horn of the spinal cord which was markedly reduced by dorsal rhizotomy, suggesting Narp is trafficked to the dorsal horn from DRG neurons. This pattern of Narp localization in axons and terminals is also consistent with previous studies that have demonstrated that Narp, which is a secreted protein, is trafficked down axons to terminals in other pathways, e.g. mossy fibers of dentate granule cells (Reti et al., 2002b) and to vasopressin terminals in the posterior pituitary (Reti et al., 2008a). Moreover, electron microscopy studies have also shown that vasopressin (Reti et al., 2008a) and orexin (I.M. Reti, R.S. Petralia, P.F. Worley, J.M. Baraban, unpublished observations) each co-localize with Narp in synaptic terminals and vesicles. Complementing these co-localization studies, we have found that the same physiological stimuli which trigger vasopressin release from the posterior pituitary also trigger Narp release into blood. Thus, taken together, these studies indicate that Narp is co-released with neuropeptides in several pathways. In this study, we have observed co-localization of Narp with CGRP providing another example of this pattern. Of note, Narp is also expressed in IB4-positive neurons, which are considered to be non-peptidergic. Accordingly, it would be interesting to determine if Narp is co-released with another neuromodulator from those neurons.

As AMPA receptors mediate transmission of nociceptive signals in the dorsal horn under basal conditions and have also been implicated in inducing pain hypersensitivity, we hypothesized Narp KO mice would display abnormal pain responses. Accordingly, we were surprised to find Narp KO mice failed to show abnormal pain responses in a variety of acute and chronic pain assays triggered by heat, pressure and inflammation. The lack of change in the spared nerve injury model is particularly interesting, given the suggestion that microglial activation plays an important role in neuropathic pain following nerve injury (Tsuda et al 2003; Coull et al 2005). It might therefore have been expected that the exaggerated microglial response would have been associated with increased allodynia.

The negative behavioral findings prompted us to assess whether Narp, like other pentraxins, may regulate inflammation. To this end, we checked whether Narp deletion altered microglia/macrophage activation following sciatic nerve transection. Using Iba1 as a marker, we found overall levels of microglia/macrophage activation were significantly increased in the dorsal horn of Narp KO mice compared with controls 3 days after transection. We also counted the number of microglia/macrophages in the same region and

found they were also significantly increased by Narp deletion, suggesting that the increased Iba1 staining intensity in Narp KO mice may be due in part to increased proliferation, survival or recruitment of microglia/macrophages in the dorsal horn. Accordingly, we performed double staining of Iba1 and BrdU to assess the possibility that Narp deletion may affect the proliferation of microglia/macrophages. However, we did not observe a significant difference in the proportion of BrdU-positive microglia/macrophages in the dorsal horns of the Narp KO and WT control mice 72 hours post-surgery. This suggests that increased proliferation of microglia/macrophages does not fully explain the phenotype observed in the Narp KO mice. Rather, our data indicates that both proliferating and non-proliferating microglia/macrophages are similarly increased by Narp deletion. We next checked whether elevated MCP1 levels in spinal cord of Narp KO mice might explain their enhanced microglial activation following SNT, as MCP1 mediates microglial activation after peripheral nerve injury (Zhang et al., 2007). However, we did not find MCP1 levels after SNT were significantly higher in the Narp KO compared with control mice either at 48 or 72 hours after surgery. There was a trend for higher MCP1 levels in the Narp KO, including at the 72 hour time point, however this difference was not significant. Accordingly, our findings raise the possibility that Narp mediates microglia/macrophage activation and/or migration via an MCP1 independent signaling pathway. One possibility is that Narp released from terminals in the dorsal horn could act directly on microglia as these cells are known to express AMPA receptors (Pocock and Kettenmann, 2007) which regulate microglial migration (Liu et al., 2009).

In summary, we have found Narp is expressed in primary nociceptive neurons. Although we did not detect effects of Narp deletion on a standard panel of pain-related behavioral assays, we found that Narp KO mice displayed an exaggerated microglia/macrophage response to SNT compared with wild type mice. These findings support the interesting possibility that Narp, and possibly other neuronal pentraxins, share with peripheral pentraxins the ability to regulate immune responses.

Acknowledgments

This work was supported by RO1DA016303. RSP was supported by the NIDCD Intramural Research Program. We thank Dr. Ya-Xian Wang for help with the immunogold studies. All authors declare no conflict of interest.

References

Allen JW, Yaksh TL. Assessment of acute thermal nociception in laboratory animals. Methods Mol Med. 2004a; 99:11–23. [PubMed: 15131325]

Allen JW, Yaksh TL. Tissue injury models of persistent nociception in rats. Methods Mol Med. 2004b; 99:25–34. [PubMed: 15131326]

Bottazzi B, Garlanda C, Salvatori G, Jeannin P, Manfredi A, Mantovani A. Pentraxins as a key component innate immunity. Current opinion in immunology. 2006; 18:10–15. [PubMed: 16343883]

Cho RW, Park JM, Wolff SBE, Xu D, Hopf C, Kim JA, Reddy RC, Petralia RS, Perin MS, Linden DJ, Worley PF. mGluR1/5-Dependent long-term depression requires the regulated ectodomain cleavage of neuronal pentraxin NPR by TACE. Neuron. 2008; 57:858–871. [PubMed: 18367087]

Coull JA, Beggs S, Boudreau D, Boivin D, Tsuda M, Inoue K, Gravel C, Salter MW, De Koninck Y. BDNF from microglia causes the shift in neuronal anion gradient underlying neuropathic pain. Nature. 2005; 438:1017–21. [PubMed: 16355225]

Date Y, Mondal MS, Matsukura S, Nakazato M. Distribution of orexin-A and orexin-B (hypocretins) in the rat spinal cord. Neurosci Lett. 2000; 288:87–90. [PubMed: 10876067]

Decosterd I, Woolf CJ. Spared nerve injury: an animal model of persistent peripheral neuropathic pain. Pain. 2000; 87:149–158. [PubMed: 10924808]

Donnelly DJ, Gensel JC, Ankeny DP, van Rooijen N, Popovich PG. An efficient and reproducible method for quantifying macrophages in different experimental models of central nervous system pathology. J Neurosci Methods. 2009; 181:36–44. [PubMed: 19393692]

Fatemi A, Wilson MA, Phillips AW, McMahon MT, Zhang J, Smith SA, Arauz EJ, Falahati S, Gummadavelli A, Bodagala H, Mori S, Johnston MV. In vivo magnetization transfer MRI shows dysmyelination in an ischemic mouse model of periventricular leukomalacia. J Cereb Blood Flow Metab. 2011; 31:2009–18. [PubMed: 21540870]

Garlanda C, Bottazzi B, Bastone A, Montovani A. Pentraxins at the crossroads between innate immunity, inflammation, matrix deposition, and female fertility. Annu Rev Immunol. 2005; 23:337–66. [PubMed: 15771574]

Guan JL, Wang QP, Shioda S. Immunoelectron microscopic examination of orexin-like immunoreactive fibers in the dorsal horn of the rat spinal cord. Brain Res. 2003; 987:86–92. [PubMed: 14499949]

Hargreaves K, Dubner R, Brown F, Flores C, Joris J. A new and sensitive method for measuring thermal nociception in cutaneous hyperalgesia. Pain. 1988; 32:77–88. [PubMed: 3340425]

He BP, Tay SS, Leong SK. Microglia responses in the CNS following sciatic nerve transection in C57BL/Wld(s) and BALB/c mice. Exp Neurol. 1997; 146:587–95. [PubMed: 9270072]

Johnson AW, Crombag HS, Takamiya K, Baraban JM, Holland PC, Huganir RL, Reti IM. A selective role for neuronal activity regulated pentraxin in the processing of sensory-specific incentive value. J Neurosci. 2007; 27:13430–5. [PubMed: 18057201]

Lawson SN, Waddell PJ. Soma neurofilament immunoreactivity is related to cell size and fibre conduction velocity in rat primary sensory neurons. J Physiol. 1991; 435:41–63. [PubMed: 1770443]

Lee GW, Lee TH, Vilcek J. TSG-14, a tumor necrosis factor- and IL-1-inducible protein, is a novel member of the pentraxin family of acute phase proteins. Journal of Immunology. 1993; 150:1804–12.

Lee TH, Lee GW, Ziff EB, Vilcek J. Isoloation and characterization of eight tumor necrosis factor-induced gene sequences from human fibroblasts. Molecular Cell Biology. 1990; 10:1982–88.

Liu L, Rudin M, Kozlova EN. Glial cell proliferation in the spinal cord after dorsal rhizotomy or sciatic nerve transection in the adult rat. Exp Brain Res. 2000; 131:64–73. [PubMed: 10759172]

Liu GJ, Nagarajah R, Banati RB, Bennett MR. Glutamate induces directed chemotaxis of microglia. Eur J Neurosci. 2009; 29:1108–18. [PubMed: 19302147]

Marnell L, Mold C, Du Clos TW. C-reactive protein: Ligands, receptors, and role in inflammation. Clincal Immunology. 2005; 117:104–111.

Molliver DC, Wright DE, Leitner ML, Parsadanian AS, Doster K, Wen D, Yan Q, Snider WD. IB4-binding DRG neurons switch from NGF to GDNF dependence in early postnatal life. Neuron. 1997; 19:849–861. [PubMed: 9354331]

Nagy GG, Al-Ayyan M, Andrew D, Fukaya M, Watanabe M, Todd AJ. Widespread expression of the AMPA receptor GluR2 subunit at glutamatergic synapses in the rat spinal cord and phosphorylation of GluR1 in response to noxious stimulation revealed with an antigen-unmasking method. J Neurosci. 2004; 24:5766–77. [PubMed: 15215299]

O'Brien RJ, Xu DS, Petralia RS, Steward O, Huganir RL, Worley P. Synaptic clustering of AMPA receptors by the extracellular immediate-early gene product Narp. Neuron. 1999; 23:309–323. [PubMed: 10399937]

Pocock JM, Kettenmann H. Neurotransmitter receptors on microglia. Trends Neurosci. 2007; 30:527–35. [PubMed: 17904651]

Reti IM, Baraban JM. Sustained increase in Narp protein expression following repeated electroconvulsive seizure. Neuropsychopharmacology. 2000; 23:439–43. [PubMed: 10989271]

Reti IM, Minor LB, Baraban JM. Selective expression of Narp in central vestibular pathways: dependence on sensory input. European Journal of Neuroscience. 2002a; 16:1949–58. [PubMed: 12453059]

Reti IM, Reddy R, Worley PF, Baraban JM. Prominent Narp expression in projection pathways and terminal fields. Journal of Neurochemistry. 2002b; 82:935–44. [PubMed: 12358799]

Reti IM, Reddy R, Worley PF, Baraban JM. Selective expression of Narp, a secreted neuronal pentraxin, in orexin neurons. Journal of Neurochemistry. 2002c; 82:1561–5. [PubMed: 12354306]

Reti IM, Miskimon M, Dickson M, Petralia RS, Takamiya K, Bland R, Saini J, During MJ, Huganir RL, Baraban JM. Activity-dependent secretion of neuronal activity regulated pentraxin from vasopressin neurons into the systemic circulation. Neuroscience. 2008a; 151:352–60. [PubMed: 18082971]

Reti IM, Crombag HS, Takamiya K, Sutton JM, Guo N, Dinenna ML, Huganir RL, Holland PC, Baraban JM. Narp regulates long-term aversive effects of morphine withdrawal. Behav Neurosci. 2008b; 122:760–8. [PubMed: 18729628]

Tao YX. Dorsal horn alpha-amino-3-hydroxy-5-methyl-4-isoxazolepropionic acid receptor trafficking in inflammatory pain. Anesthesiology. 2010; 112:1259–65. [PubMed: 20395828]

Tillet WS, Francis T Jr. Serological reactions in pneumonia with a non protein somatic fraction of pneumococcus. Journal of Experimental Medicine. 1930; 52:561–85. [PubMed: 19869788]

Tsuda M, Shigemoto-Mogami Y, Koizumi S, Mizokoshi A, Kohsaka S, Salter MW, Inoue K. P2X4 receptors induced in spinal microglia gate tactile allodynia after nerve injury. Nature. 2003; 424:778–83. [PubMed: 12917686]

Tsui CC, Copeland NG, Gilber DJ, Jenkins NA, Barnes C, Worley P. Narp, a novel member of the pentraxin family, promotes neurite outgrowth and is dynamically regulated by neuronal activity. Journal of Neuroscience. 1996; 16:2463–2478. [PubMed: 8786423]

Woolfe G, MacDonald AD. The evaluation of the analgesic action of pethidine hydrochloride (Demerol). J Pharmacol Exp Ther. 1944; 80:300.

Xu D, Hopf C, Reddy R, Cho RW, Guo L, Lanahan A, Petralia RS, Wenthold RJ, O'Brien RJ, Worley P. Narp and NP1 form heterocomplexes that function in developmental and activity-dependent synaptic plasticity. Neuron. 2003; 39:513–528. [PubMed: 12895424]

Zhang J, Shi XQ, Echeverry S, Mogil JS, De Koninck Y, Rivest S. Expression of CCR2 in both resident and bone marrow-derived microglia plays a critical role in neuropathic pain. J Neurosci. 2007; 27:12396–406. [PubMed: 17989304]

Highlights

- Narp is expressed in small neurons of the dorsal root ganglia.
- Narp is expressed in IB4- and CGRP-positive neurons, markers of nociceptive neurons.
- Mice are unaffected by Narp deletion on a panel of standard pain behavioral assays.
- Narp KO mice show an enhanced microglia/macrophage response following sciatic nerve transection.

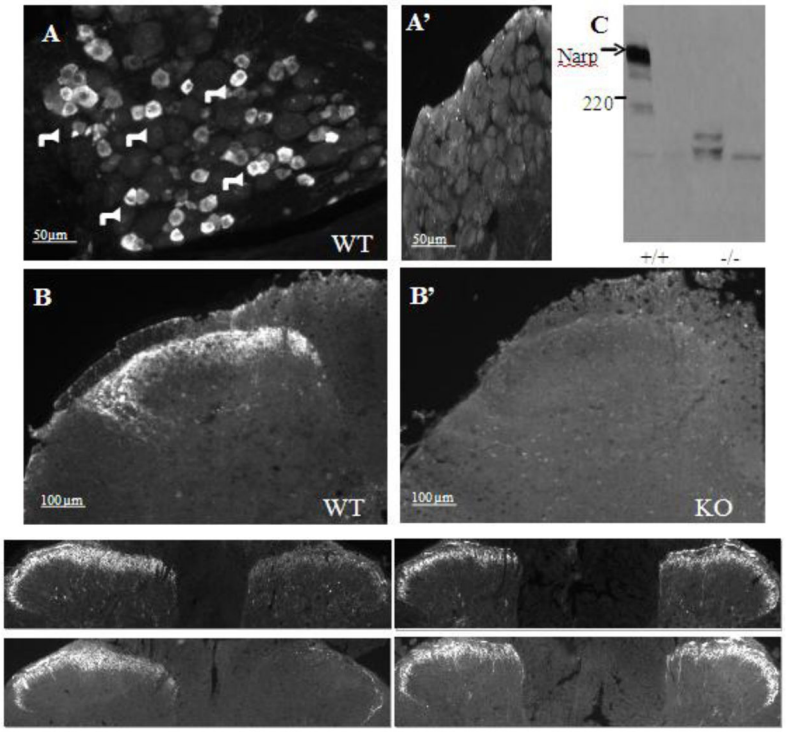

Figure 1.

Narp immunoreactivity in dorsal root ganglia and spinal cord. (A) Fluorescent immunostaining of DRG from naïve WT mice reveals Narp expression present predominantly in small diameter neurons, indicated by arrows. (B) Narp staining labels external laminae of dorsal horn. Specificity of staining is confirmed by absence of Narp staining in KO DRG (A') and spinal cord (B'). (C) Western blot probed with Narp antibody shows DRG lysates from a Narp KO and WT control mouse. The Narp antibody recognizes a high molecular weight complex that is absent in the Narp KO mouse. (D–E) Fluorescent immunostaining in rat spinal cord after rhizotomy at L4 to L6 showing Narp (D) and CGRP (D') expression at L5 spinal cord, and Narp (E) and CGRP (E') expression at the T12 segment. The side ipsilateral to surgery is indicated by asterisk.

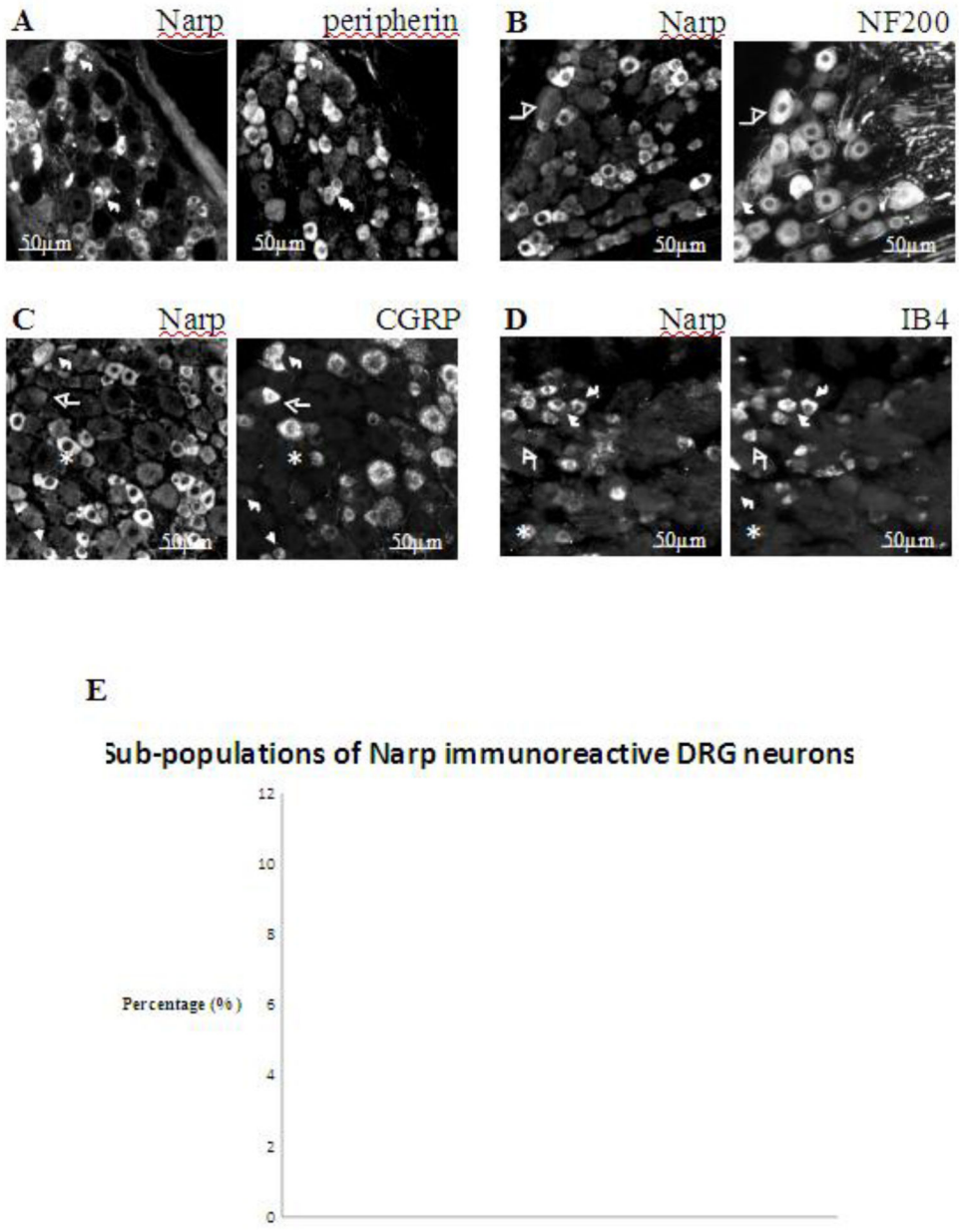

Figure 2.

Characterization of Narp immunoreactive DRG neurons. Fluorescent photomicrographs of naïve mouse lumbar (L4 to L6) DRG show Narp double-staining with peripherin (A), NF200 (B), CGRP (C), and IB4-binding (D). Short arrows highlight neurons that co-express Narp and marker. Asterisks highlight neurons that only express Narp. Long arrows highlight neurons that only express marker. (E) Mean percentages of Narp immunoreactive DRG neurons expressing each of these markers.

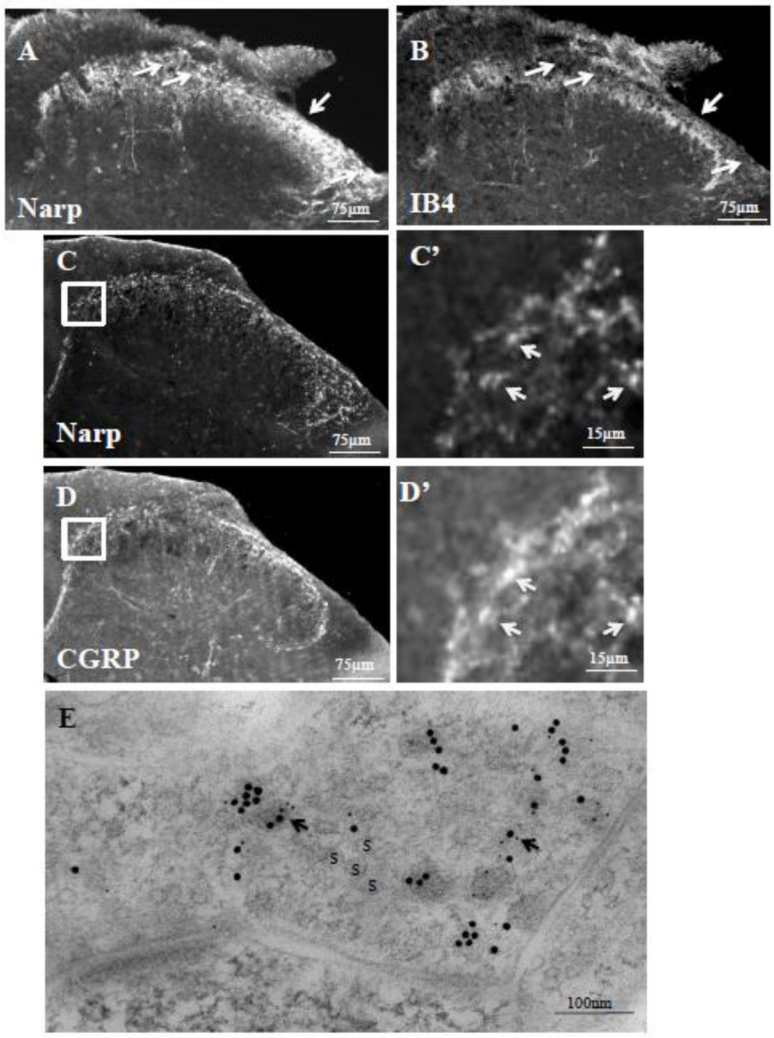

Figure 3.

Narp positive terminals in the dorsal horn. Double-label staining of mouse lumbar spinal cord for Narp (A) and IB4-binding (B) demonstrates Narp expression extending to the central lamina II of the dorsal horn. Arrows highlight lamina I where Narp but not IB4 binding is present. Double label studies of lumbar spinal cord for Narp (C) and CGRP (D) also demonstrates overlap in staining. Boxed areas are shown at higher power. Arrows point to Narp immunoreactive puncta (C') that overlap with CGRP immunoreactive puncta (D'). (E) Double-label electron microscopic immunogold study of Narp (small gold particles) and CGRP (large gold particles) in a synaptic terminal. S–synaptic vesicle

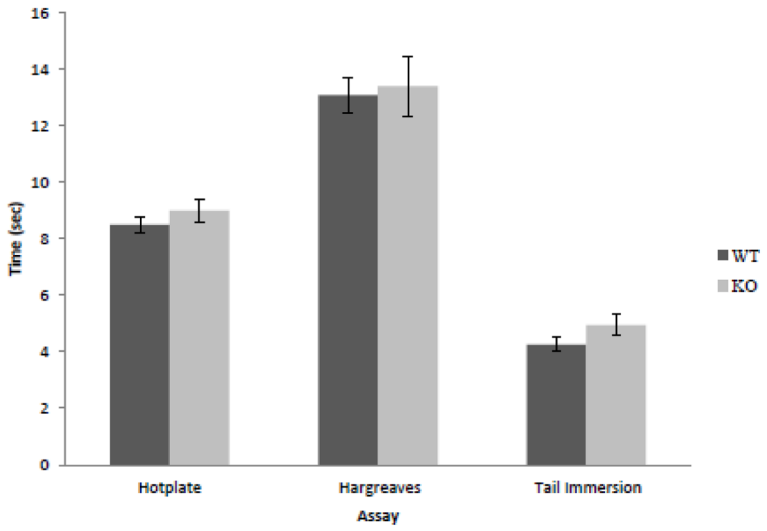

Figure 4.

Effect of Narp deletion on nociceptive responses. Mean response times to thermal stimuli in the hotplate (WT: n=20; KO: n=21), Hargreaves (n=10 in each group), and tail immersion assays (n=16 in each group).

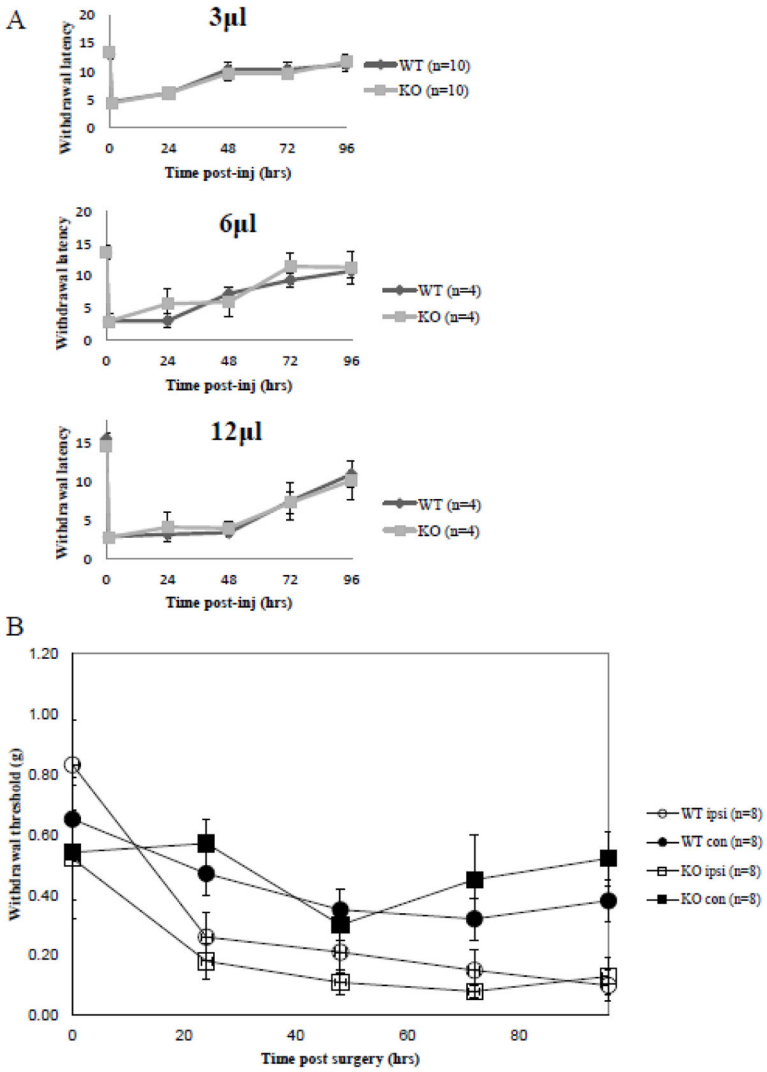

Figure 5.

Responses to inflammatory and neuropathic pain. (A) Thermal sensitivity following CFA plantar injection was monitored using the Hargreaves method following plantar injections of a 1:1 mixture of CFA:normal saline in volumes of 3, 6 or 12 microliters. (B) Mechanical hypersensitivity was assessed with von Frey filaments following spared nerve injury.

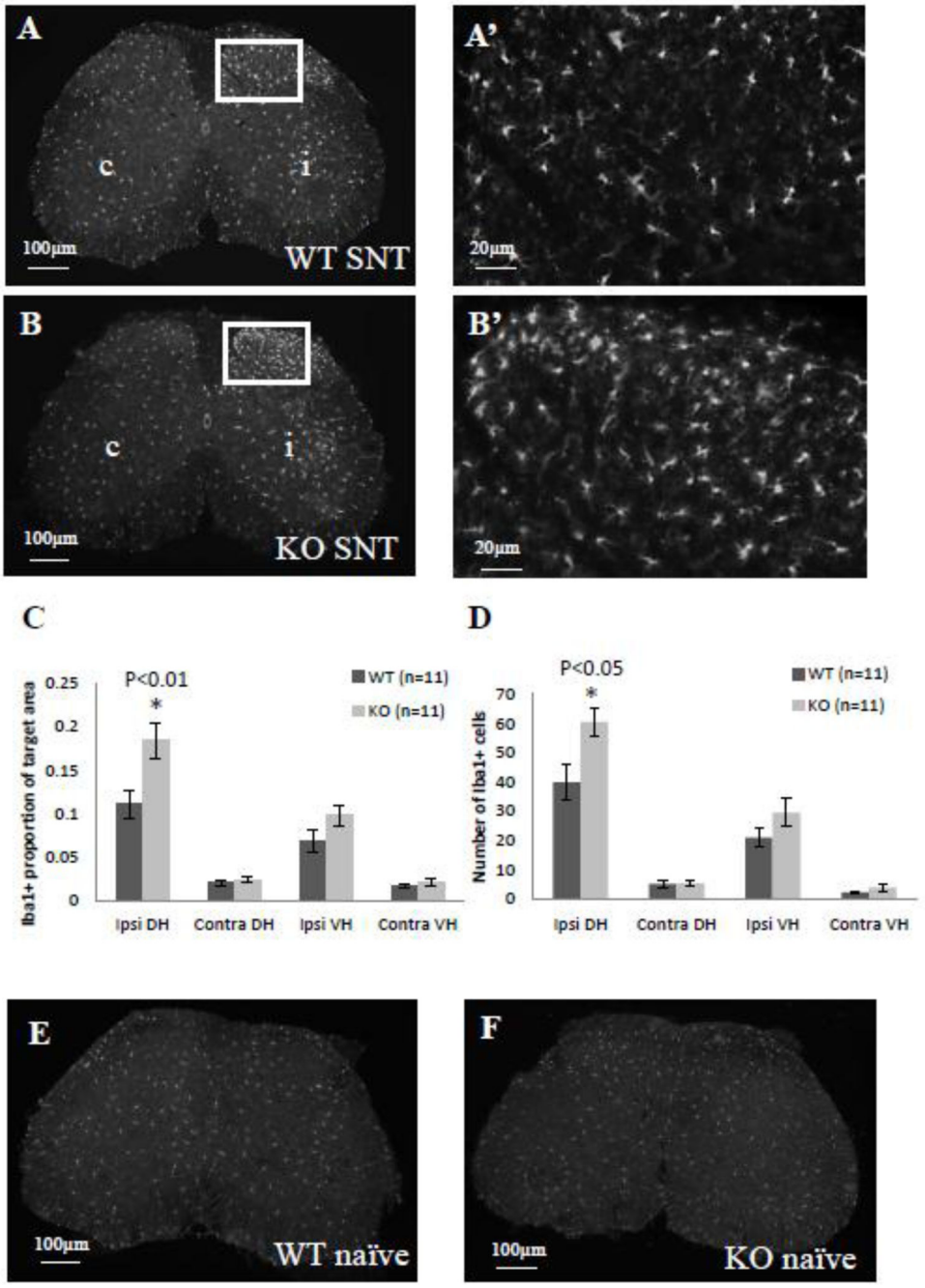

Figure 6.

Microglial activation after sciatic nerve transection. Iba1 staining in lumbar (L4–5) spinal cord of WT (A) and Narp KO (B) mice 3 days after unilateral sciatic nerve transection (SNT). Boxed areas are shown at higher power (A' and B'). c = contralateral. i = ipsilateral. Mean proportion of area that is Iba1-positive (C) and mean Iba1-positive cell count (D) in each of four quadrants of spinal cord. Asterisks highlight a significant difference in Iba1 staining intensity (C) and cell count (D) in the ipsilateral dorsal horn of Narp KO compared

with WT mice. Errors bars indicate SEM. Iba1 staining in lumbar spinal cord of naive WT (E) and Narp KO (F) mice.

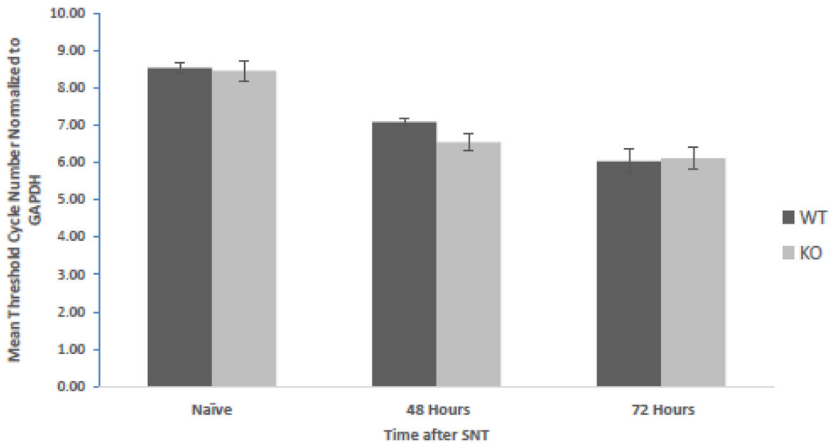

Figure 7.

MCP1 mRNA levels in the spinal cord after sciatic nerve transection. Spinal cord samples were obtained from WT and Narp KO mice 48 or 72 hours after transection, as well as from naïve mice (6 mice in each group). mRNA levels were quantified by qPCR. The graph shows the mean cycle number, C_t, for each condition normalized to GAPDH. Error bars indicate SEM.